Angewandte Chemie
Eine Zeitschrift der Gesellschaft Deutscher Chemiker

Supporting Information



69451 Weinheim, Germany

# Gadolinium(III) Spin Labels for High-Sensitivity Distance Measurements in Transmembrane Helices**

*Erez Matalon, Thomas Huber, Gregor Hagelueken, Bim Graham, Veronica Frydman, Akiva Feintuch, Gottfried Otting, and Daniella Goldfarb**

anie_201305574_sm_miscellaneous_information.pdf

**Materials.** The phospholipid 1,2-dioleoyl-*sn*-glycero-3-phosphocholine (DOPC) was purchased from *Avanti Polar Lipids* Inc. (Alabaster, AL, USA). MTSSL (1-oxyl-2,2,5,5-tetramethyl-3 pyrroline-3-methyl) methanethiosulfonate was purchased from Toronto Research Chemicals (Ontario, CA, USA). The C1 tag loaded with $Gd^{3+}$ was synthesized according to a previously published protocol.[1] The DOTA tag loaded with $Gd^{3+}$ was likewise synthesized according to a previously published protocol.[2]

**Peptide purification and labeling.** The WALP peptides were purchased from LifeTein LLC (South Plainfield, NJ, USA). The peptides were labeled by formation of a disulfide bridge. A 10-fold excess of the spin label dissolved in DMSO was used for labeling. The spin labels, together with the peptide in DMSO, were stirred at room temperature for 12 h. Spin-labeled peptides were purified by HPLC on a C4 reverse phase column (Vydac 214TP1010). Labeled peptides were shown to be homogeneous by analytical HPLC (>97%, by weight). The labeling was confirmed by electrospray mass spectroscopy.

**Preparation of samples for EPR measurements.** EPR samples were prepared by mixing the peptide and phospholipids stock solution to give a WALP-to-phospholipids molar ratio of 1:1000. A low peptide-to-ligand ratio minimizes the effective local tag concentration in the membrane, which would be detrimental for DEER measurements.[3] WALP peptides, dissolved in a 2:1 (v/v) $CHCl_3$/MeOH mixture at a concentration of 50 μM, were added to the phospholipids solution in 2:1 $CHCl_3$/MeOH. The lipid-peptide solution was dried using a nitrogen gas stream followed by drying in vacuum overnight. Multi-lamellar vesicles (MLV) were prepared by hydrating the peptide-lipid film in 80 μL of 100 mM deuterated phosphate buffer at pH 7.2. The suspension was mixed using a vortex mixer for 2 min. 20% (by volume) glycerol-$d_8$ was added to the sample. Deuterated solvents were used in order to extend the phase memory time $T_m$. Glycerol is commonly used to prevent ice formation and vesicle aggregation upon freezing.[4, 5]

For X-band DEER measurements, approximately 50-60 μL of equilibrated sample were rapidly frozen by insertion of the EPR Teflon tube (2.7 mm i.d. and 3.7 mm o.d.) into liquid nitrogen. For W-band DEER measurements, about 3 μL of the sample were rapidly frozen by inserting the samples into W-band tubes (0.6 mm i.d. and 0.84 mm o.d., VitroCom Inc. Mountain Lakes, NJ, USA) followed by rapid freezing in liquid nitrogen. The samples were stored in liquid nitrogen until measured.

**CW-EPR measurements.** All CW X-band (9.5 GHz) measurements were performed at room temperature (22-25 °C) on a Bruker ELEXSYS 500 EPR spectrometer.

**DEER measurements**. The four-pulse DEER sequence was used for all DEER measurements. X-band measurements were carried out at 50 K on a Bruker ELEXSYS E580 EPR spectrometer (9.5 GHz) using a ER4118X-MS-5X probe head with a split ring resonator (5 mm sample access). Both π pulses of the

observer channel were set to 32 ns. The π pulse of the pump channel was set to 16 ns. A 2-step phase cycling was applied to the first π/2 pulse. The pump frequency was set to the maximum of the EPR spectrum and the observe frequency was 65 MHz higher. The repetition delay was 2.5 ms. The accumulation time for the measurement was about 16 h.

The W-band DEER measurements were carried out on a home-built EPR spectrometer[7, 8] at 10 K. The pump and observe frequencies were separated by 75 MHz and the observe π/2 and π pulses were 20 and 40 ns long, respectively. The pump pulse duration was 15 ns. The repetition delay was 500 μs and accumulation times were about 1.5-10 h and. A four-step phase cycle was employed: $\pi/2_{obs}$: +x, -x, +x, -x; $\pi_{obs}$: +x, +x, -x, -x; $\pi_{pump}$: +x, +x, +x, +x; $\pi_{obs}$: +x, +x, +x +x. The receiver phase cycle was +, -, +, -. The phase cycling was needed to remove instrumental artifacts and to compensate for pulse imperfections.

The DEER data were analyzed using the program DeerAnalysis 2011.[6] Distance distributions were obtained using a single Gaussian function for WALP23-NO and Tikhonov regularization with a regularization parameter of 100 for the WALP-C1 and WALP-DOTA series.

W-band echo-detected (ED) EPR spectra of the samples with $Gd^{3+}$ tags were recorded at 10 K using π/2 and π pulse durations of 30 ns and 60 ns, respectively, with an echo delay of 500 ns and a repetition time of 1 ms.

Echo decays of the samples with $Gd^{3+}$ tags were measured by Hahn echo decay experiments (π/2-τ-π-τ-*echo*) with the spectrometer frequency positioned at the observe frequency. The π/2 and π pulse durations were 30 ns and 60 ns, respectively (Figure S2). The measurements were performed at 10 K with a repetition time of 1 ms and two-step phase cycling. For WALP-NO the same sequence with pulse durations of 16 ns (π/2) and 32 ns (π). The field position was at the maximum echo intensity and measurement was performed at 50 K.

**CW-EPR of nitroxide spin-labeled WALP23**

Room temperature X-band CW-EPR spectra of MTSSL labeled WALP23 (WALP23-NO) showed that the addition of 20% glycerol to the MLV solutions did not affect the spectrum, suggesting that the membrane properties were maintained. The spectrum also showed that the peptide was incorporated, as demonstrated by the slow tumbling rate of the label evidenced by the line broadening in the EPR spectrum.[9] The peptide is insoluble in aqueous solutions without detergents.

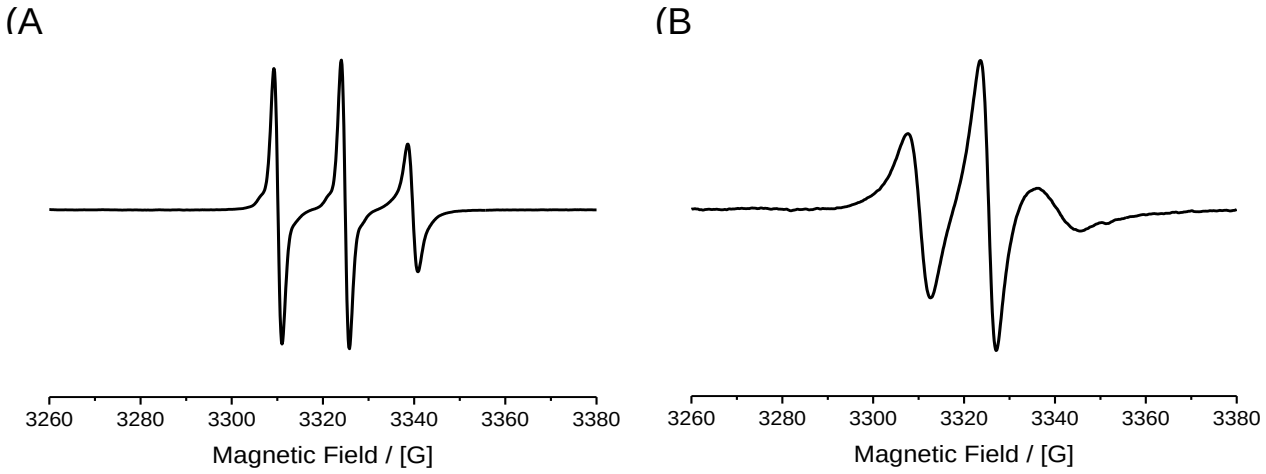


**Figure S1.** X-band room temperature CW-EPR spectra of WALP23 doubly labeled with nitroxide tags, (A) in a DMSO solution and (B) in DOPC MLV in $D_2O$. The spectra were normalized to the maximal amplitude of the $M_I = 0$ transition.

## Echo decay measurements

A comparison between the echo decays of WALP23-NO, WALP23-C1 and WALP23-DOTA shows that WALP-DOTA has the longest decay. Because the decays are not exponential we chose to characterize them by the interval τ at which the echo decayed to 10% of its value for τ=250 ns, $\tau_{10\%}$. This is usually the maximal time at which DEER measurements are still possible so it is a significant number for optimizing DEER measurements and assessing the sensitivity. A list of all the $\tau_{10\%}$ values for the different peptides is given in Table S1. The echo decay of the $Gd^{3+}$ labeled peptides was measured with longer pulses than the observe pulses used in the DEER measurement. In the presence of instantaneous diffusion the two different power settings may lead to different echo decays. However, for the low concentrations used (0.1 mM $Gd^{3+}$) we expect negligible instantaneous diffusion.

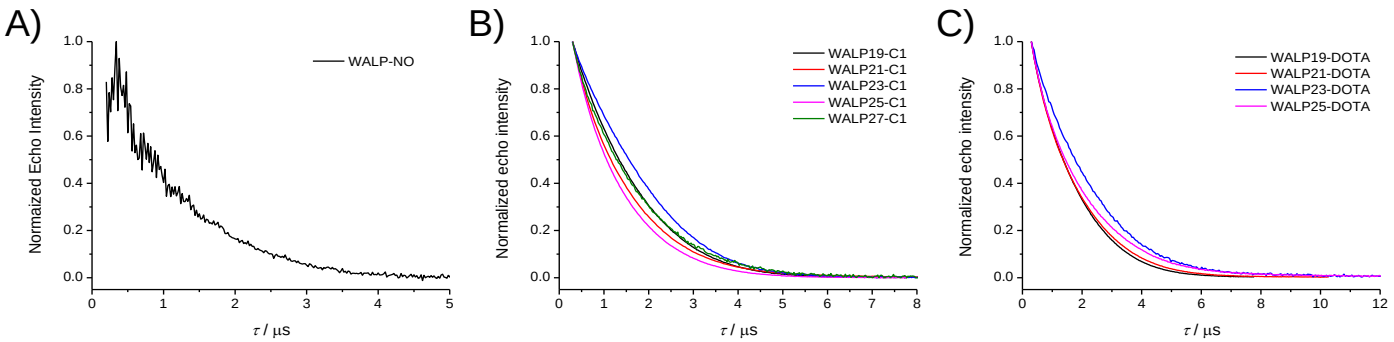


**Figure S2.** Hahn echo decay measurements of the WALP peptides studies in MLVs in $D_2O$ buffer (20% glycerol). (A) X-band echo decays of WALP23-NO. The measurements were performed at 50 K using pulse durations of 16 ns (π/2) and 32 ns (π). (B) and (C) W-band echo decays of WALP-C1 and WALP-DOTA measured at the field position of the observe pulses. The measurements were performed at 10 K using pulse durations of 30 ns (π/2) and 60 ns (π).

***Table S1.*** $\tau_{10\%}$ values for the WALP peptides labeled with different tags

| **Peptide** | **$\tau_{10\%}$ (μs)** | | |
|---|---|---|---|
| | $Gd^{3+}$-DOTA | $Gd^{3+}$-C1 | MTSSL |
| WALP19 | 3.5 | 3.3 | - |
| WALP21 | 3.8 | 3.1 | - |
| WALP23 | 4.5 | 3.6 | 2.5 |
| WALP25 | 4.2 | 2.8 | - |
| WALP27 | - | 3.4 | - |

**Sensitivity considerations**

The absolute sensitivity of the W-band $Gd^{3+}$-$Gd^{3+}$ DEER on WALP23-C1 and WALP23-DOTA is considerably larger X-band DEER measurements on WALP23-NO. This stems primarily from the huge difference in sample amount (factor ~ 20), longer echo decay and the faster repetition rate. To give a more quantitative estimation of the better sensitivity, we calculated the DEER SNR per nmol peptide per 1 h data accumulation for all these samples according to:

$$SNR \propto \frac{\lambda}{noise \cdot C}$$

where *noise* is the noise amplitude of the normalized DEER traces, λ is the measured modulation depth parameter, and *C* is the nominal number of nmols. The obtained SNR's are shown in Table 2S.

***Table 2S.*** DEER SNR of WALP23 labeled with different tags

| **Peptide** | **SNR** |
|---|---|
| WALP23-NO | 0.5±1 |
| WALP23-DOTA | 20±4 |
| WALP23-C1 | 50±3 |

The SNR values listed in Table S2 clearly reveal above an order of magnitude difference in absolute sensitivity. However, one should take these numbers only as estimates and not absolute numbers because this evaluation depends on instrumental parameters, power available, resonators used etc. The differences between WALP23-DOTA and WALP-C1, which were recorded under the same experimental conditions, can also arise from differences in the actual concentration, namely that not all peptides were inserted into the membrane. As the purpose of this work was not a systematic sensitivity study, we did not determine the yield of the peptide insertion. Also the evolution times of the different traces are different, but as the major contribution to the sensitivity comes from the samples size, the huge difference in absolute sensitivity is general.

## DEER measurement of singly labeled WALP23-C1

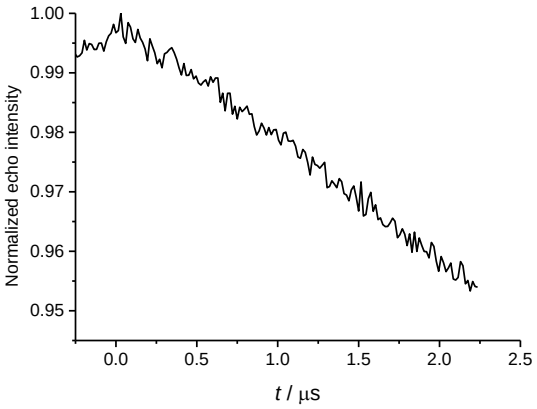


**Figure S3**. Raw W-band DEER data obtained for WALP23 singly labeled with the C1 tag at position 23 in MLVs in $D_2O$ buffer (20% glycerol) concentration ratio of peptide to lipid = 1:1000). The trace was normalized to 1. The DEER decay is linear, excluding the presence of oligomers and assuring that that the MLV environment does not promote close vicinities (within the sensitivity range of DEER) of WALP peptide due to confinement to a small volume.[10, 11]

## Raw data of DEER measurements

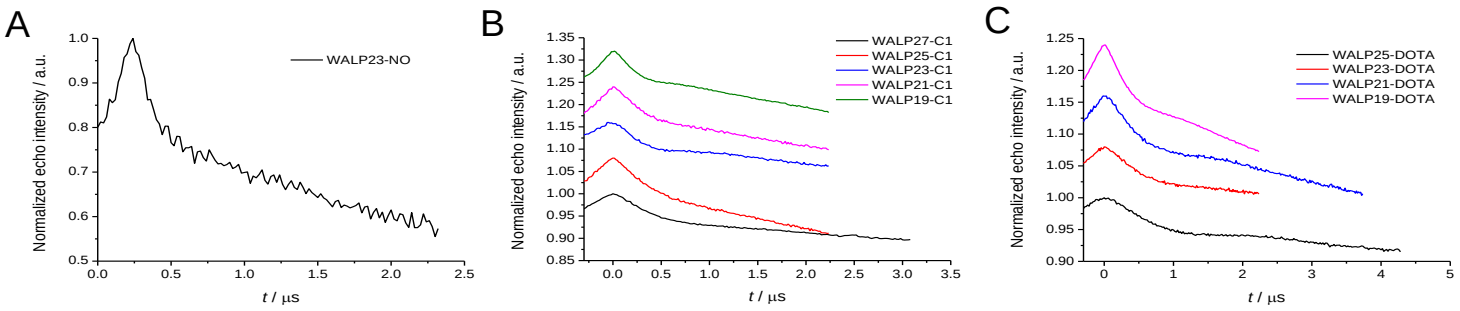


**Figure S4**. Raw data of the DEER measurements. (A) Normalized X-band DEER data obtained for WALP23-NO. (B) Normalized W-band DEER data obtained for WALPs labeled with the C1 tag shown in Figure 1C. For improved visualization, traces were shifted by 0.09 units in the vertical direction from their neighboring traces. (C) Same as (B), except for WALPs labeled with the DOTA tag, of Figure 1B. Experimental conditions: for WALP23-NO: 50 K, 32 ns observe pulses, 16 ns pump π pulse, and Δν = 65 MHz. For WALP23-C1 and WALP23-DOTA tags: 10 K, 15 ns pump pulse positioned at the maximum of the $Gd^{3+}$ central transition (|-1/2>→|1/2>), observe pulses (20, 40 ns) placed at Δν = 75 MHz from the central transition.

## MtsslWizard predictions for WALP23-NO and WALP23-DOTA

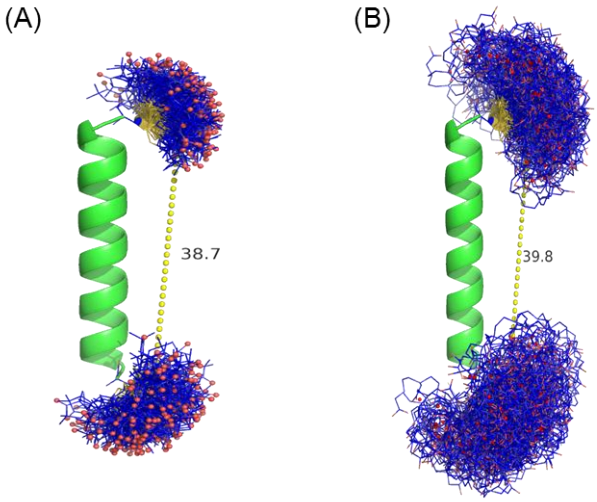


**Figure S5.** MtsslWizard predictions for WALP23-NO and WALP23-DOTA. (A) For the MTSSL labeled model (WALP23-NO), the WALP peptide (green cartoon model) was loaded into PyMOL and the two cysteine residues were labeled with MTSSL using mtsslWizard v1.1 (http://pymolwiki.org/index.php/MtsslWizard) with default settings ('vdW restraints: tight' and 'thorough search'). The figure shows all MTSSL conformations produced by the software as sticks. The oxygen of the nitroxide is displayed as red spheres. The yellow dashed line identifies the distance between the geometric averages of the label ensembles. (B) For the DOTA labeled model (WALP23-DOTA), the DOTA label (displayed as a stick model) was newly added to the mtsslWizard software.[12] The $Gd^{3+}$ ion (red spheres) was defined as the spin center for distance calculations and the linker was allowed to rotate freely around all 6 rotatable bonds. The labeling was again performed using the default settings ('vdW restraints: tight' and 'thorough search'. The distance histograms were produced using the "Measure" mode of mtsslWizard.

## Computing distance distributions between spin labels using PyParaTools

To assess the accuracy of the $Gd^{3+}$-$Gd^{3+}$ DEER distance measurements, we modeled the distance distribution by crafting the $Gd^{3+}$ C1 tag onto the cysteines in position 1 and n of the WALP peptide structure, as described previously.[13] Ideal α-helical geometry was assumed for the WALP peptide structure and 10000 conformers were generated for each label by randomly varying the $\chi_1$ and $\chi_2$ angles of the cysteine residue as well as all rotatable bonds between the cysteine sulfur atoms and the $Gd^{3+}$ chelate or the 2,2,5,5-tetramethyl-2,5-dihydro-1H-pyrrol, respectively. In difference to MtsslWizard which randomly varies torsion angles in the full range of 0 to 360 degrees, PyParaTools accounts more accurately for local torsion angle preferences in the attached labels by randomly sampling dihedral angles around rotamer states. For example, the preferred rotamer states of a disulfide bond through which a label is attached are known to be either 90 or -90 degrees, and consequently, PyParaTools samples this torsion angle randomly around these values with a window size of 20 (±10) degrees. Similarly, torsions around carbon-carbon bonds are sampled from the preferred rotamer states -60±10, 60±10 and 180±10 degrees, with the exception of the last rotatable bond to the $Gd^{3+}$ chelate or the 2,2,5,5-tetramethyl-2,5-dihydro-1H-pyrrol which are assumed to be freely rotatable or restricted to -90±10 / 90±10 degrees, respectively. Models with van der Waals violations between the tags and the protein were removed, resulting in approximately 3000 C1-$Gd^{3+}$ tag conformations at residue position 1, 1000 C1-$Gd^{3+}$ tag conformations at residue position n, 5000 MTSL tag conformations at residue position 1, and 2000 MTSL tag conformations at residue position n. For each pair-wise combination of modeled tag conformations, the distance between paramagnetic centers was calculated, and the resulting $3 \cdot 10^6$ to $10^7$ distances tallied into distributions with 0.1 nm bin widths.

## C1 tag rotamer structure for different WALP peptides

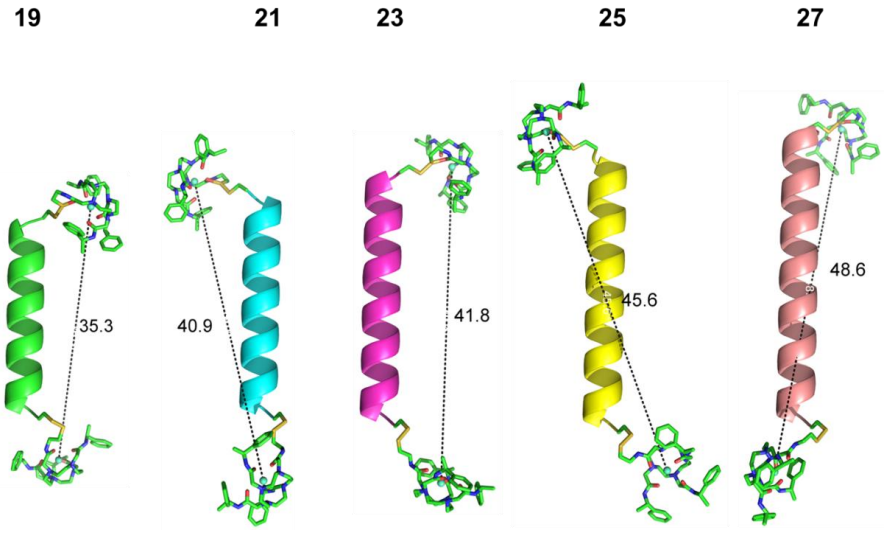


**Figure S6.** Models of WALP peptides labeled with C1-$Gd^{3+}$ tags, with the indicated metal-metal distance equal to the most abundant distance in the distribution calculated from more than $3 \cdot 10^6$ physically possible models as shown in Figure 3.

## Helical wheel diagram

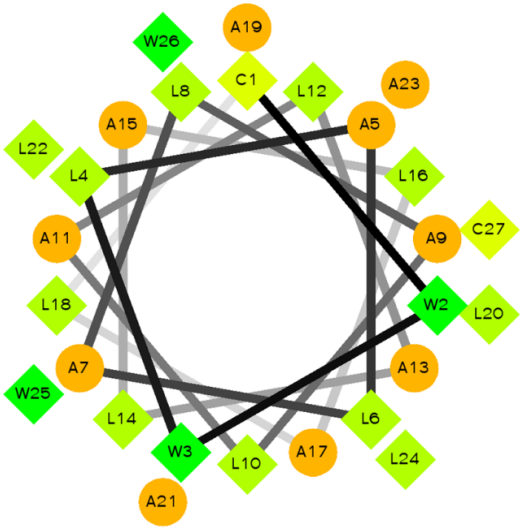


**Figure S7.** Helical wheel projection of WALP27 [taken from: http://rzlab.ucr.edu/scripts].

## Summary of modeling results for $Gd^{3+}$ tags

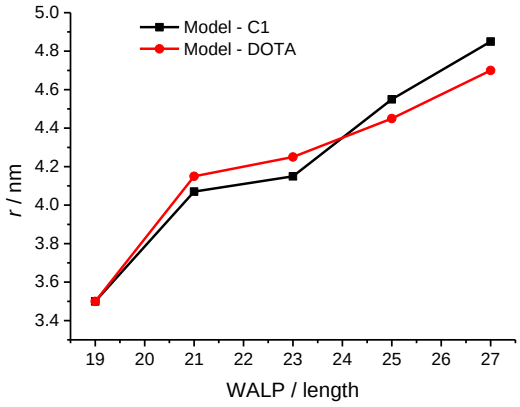


**Figure S8.** Comparison of the most abundant distances obtained from the models calculated for different WALPs using the C1-$Gd^{3+}$ and DOTA-$Gd^{3+}$ tags.

## References


[1] B. Graham, C. T. Loh, J. D. Swarbrick, P. Ung, J. Shin, H. Yagi, X. Jia, S. Chhabra, N. Barlow, G. Pintacuda, T. Huber, G. Otting, *Bioconjugate Chem.* **2011**, *22*, 2118-2125.

[2] D. Thonon, V. Jacques, J. F. Desreux, *Contrast Media Mol. Imaging* **2007**, *2*, 24-34.

[3] R. Dastvan, B. E. Bode, M. P. R. Karuppiah, A. Marko, S. Lyubenova, H. Schwalbe, T. F. Prisner, *J. Phys. Chem. B* **2010**, *114*, 13507-13516.

[4] T. J. Anchordoguy, A. S. Rudolph, J. F. Carpenter, J. H. Crowe, *Cryobiology* **1987**, *24*, 324-331.

[5] E. R. Georgieva, A. S. Roy, V. M. Grigoryants, P. P. Borbat, K. A. Earle, C. P. Scholes, J. H. Freed, *J. Magn. Reson.* **2012**, *216*, 69-77.

[6] G. Jeschke, V. Chechik, P. Ionita, A. Godt, H. Zimmermann, J. Banham, C. R. Timmel, D. Hilger, H. Jung, *Appl. Magn. Reson.* **2006**, *30*, 473-498.
[7] D. Goldfarb, Y. Lipkin, A. Potapov, Y. Gorodetsky, B. Epel, A. M. Raitsimring, M. Radoul, I. Kaminker, *J. Magn. Reson.* **2008**, *194*, 8-15.
[8] I. Gromov, V. Krymov, P. Manikandan, D. Arieli, D. Goldfarb, *J. Magn. Reson.* **1999**, *139*, 8-17.
[9] J. H. Freed, (Ed.: J. L. Berliner), Academic Press, New York, **1976**, pp. 53-132.
[10] E. Matalon, I. Kaminker, H. Zimmermann, M. Eisenstein, Y. Shai, D. Goldfarb, *J. Phys. Chem. B* **2013**, 117, 2280-2293.
[11] S. Ruthstein, A. Potapov, A. M. Raitsimring, D. Goldfarb, *J. Phys. Chem. B* **2005**, 109, 22843-22851.
[12] G. Hagelueken, D. Abdullin, R. Ward, O. Schiemann, *Mol. Phys.* **2013** (in press).
[13] I. Kaminker, H. Yagi, T. Huber, A. Feintuch, G. Otting, D. Goldfarb, *Phys. Chem. Chem. Phys.* **2012**, *14*, 4355-4358.